AGU PUBLICATIONS

JGR

Journal of Geophysical Research: Atmospheres

RESEARCH ARTICLE
10.1002/2016JD025370

Key Points:
- The effect of the Indian summer monsoon strengthens from downstream to upstream in the YTR basin
- Periodic variability of the Indian summer monsoon controls interannual nonstationary variation of precipitation in the YTR basin
- The weakening Indian summer monsoon caused precipitation decrease in the YTR basin during the recent two decades

Supporting Information:
- Supporting Information S1

Correspondence to:
Y.-F. Sang and F. Sun,
sangyf@igsnrr.ac.cn;
sunsangyf@gmail.com;
sunfb@igsnrr.ac.cn

Citation:
Sang, Y.-F., V. P. Singh, T. Gong, K. Xu, F. Sun, C. Liu, W. Liu, and R. Chen (2016), Precipitation variability and response to changing climatic condition in the Yarlung Tsangpo River basin, China, *J. Geophys. Res. Atmos.*, *121*, 8820–8831, doi:10.1002/2016JD025370.

Received 16 MAY 2016
Accepted 16 JUL 2016
Accepted article online 20 JUL 2016
Published online 4 AUG 2016

Precipitation variability and response to changing climatic condition in the Yarlung Tsangpo River basin, China

Yan-Fang Sang[1], Vijay P. Singh[2], Tongliang Gong[3], Kang Xu[4], Fubao Sun[1], Changming Liu[1], Wenbin Liu[1], and Ruizhi Chen[5]

[1]Key Laboratory of Water Cycle and Related Land Surface Processes, Institute of Geographic Sciences and Natural Resources Research, Chinese Academy of Sciences, Beijing, China, [2]Department of Biological and Agricultural Engineering and Zachry Department of Civil Engineering, Texas A&M University, College Station, Texas, USA, [3]Water Conservancy Department of the Tibet Autonomous Region, Lhasa, China, [4]State Key Laboratory of Tropical Oceanography, South China Sea Institute of Oceanology, Chinese Academy of Sciences, Guangzhou, China, [5]Pearl River Hydraulic Research Institute, Guangzhou, China

Abstract Hydroclimatic process in the Yarlung Tsangpo River (YTR) basin, a sensitive area to climate change, is obviously changing during recent years, but there has limited understanding about it. In this study, we investigated the spatiotemporal variation of precipitation over last four decades in the basin and the impact thereon of the changing Indian summer monsoon at interannual and decadal time scales. All the precipitation series have similar scaling behavior, reflecting similar climatic regime throughout the basin. However, the effect of the Indian monsoon strengthens from the downstream to upstream, causing spatial variability in the seasonal distribution of precipitation, and on this basis, the YTR basin is roughly divided into three regions: east, middle, and west. Both the occurrence times and magnitude of precipitation extremes, ranging 25–50 mm/d, are exhibiting downward trends over the last four decades, which bodes well for water disaster controls in the basin. The Indian summer monsoon index, as an intensity indicator for the Indian summer monsoon, shows a positive relationship with the summer precipitation in the YTR basin. Periodic variability of the Indian monsoon determines the interannual nonstationary fluctuations of precipitation. Especially, the weakening effect of the Indian summer monsoon has caused an obvious decrease in precipitation over the rainy season after 1998. If the Indian summer monsoon keeps weakening, the precipitation would decrease and potentially water shortage would become more severe in the basin. Effective adaptation strategy should therefore be developed proactively to handle the unfavorable water situation, which is likely to occur in the future.

1. Introduction

Climate change significantly impacts the hydrological cycle [*Chen et al*., 2005; *Sang et al*., 2013; *Chandrasekar et al*., 2013] and influences socioeconomic developments and people's lives worldwide. Fundamental to water resources management is the evaluation of the effect of climate change and the changes in the hydroclimatic system. Precipitation is critical for understanding the changes in the hydroclimatic system [*Brunetti et al*., 2006; *Willems et al*., 2012; *Wang*, 2013]. Variability in the duration and intensity of precipitation at the regional scale is often of concern when investigating climate change. Although China's average annual precipitation has not changed significantly [*Zhai et al*., 1999; *Wang et al*., 2004], regional precipitation rates now fluctuate considerably, requiring further investigation of the spatiotemporal variations of regional precipitation under the climate change [*Zhang et al*., 2009; *Xu et al*., 2008; *Sang et al*., 2012].

Located on the south of the Tibetan plateau, the Yarlung Tsangpo River (YTR) basin is one of those regions that are particularly sensitive to climate change [*Xu et al*., 2009]. Due to an average altitude above 4000 m, the Tibetan plateau hinders the westerlies and strengthens the Indian monsoon through its dynamical and thermal impacts [*Bothe et al*., 2011], which is critical for the advection of heat and moisture, and climate pattern in the Tibetan plateau [*An et al*., 2012]. The YTR basin has complex topography, geography, and hydroclimate conditions [*Xu et al*., 2006; *Nie et al*., 2012]. As shown by *Yao et al*. [2012], the stable oxygen isotope ratio in precipitation and its relationship with temperature and precipitation vary over space, based on which we know that hydroclimatic condition in the YTR basin, especially in the middle and lower YTR basin (south of 30°N), is mainly controlled by the Indian monsoon. The water resources in the basin are vital for sustaining the

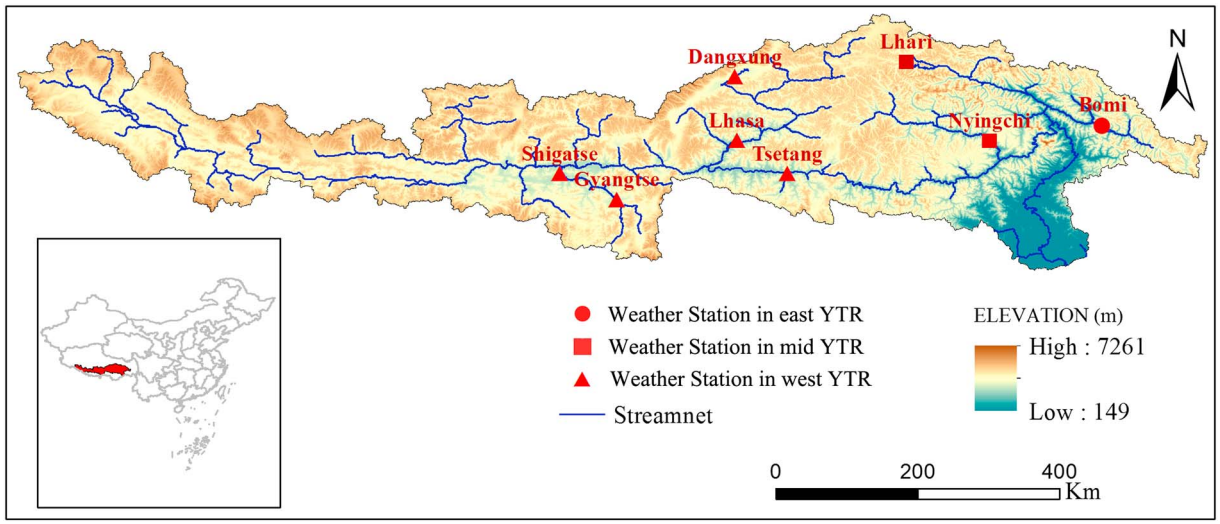

Figure 1. Locations of eight weather stations in the east, middle, and west Yarlung Tsangpo River (YTR) basin.

health of regional environmental and ecological systems and peoples' lives [*Shen*, 1986; *Li and Kang*, 2006]. In recent decades hydroclimatic processes have been observed to be changing in the basin, perhaps due to the impact of climate change [*Gao et al*., 2011; *Li et al*., 2014]. The changes directly impact the water safety of Tibet and threaten its fragile ecosystems and those who rely on them [*Klein et al*., 2004; *Wang et al*., 2008]. Further, water-related disasters occurred frequently in many small and medium size basins. The present hydroinformation systems and water conservancy facilities in the basin are not capable of handling the increasing impacts of climate change and need urgent improvement. There are many areas in the YTR basin that have sparse hydroclimatic data, which are inadequate for hydrological forecasting and meeting practical needs. Hence, people's lives in the region come under threat, and the losses caused by water-related disasters cannot be mitigated and prevented effectively.

Understanding the precipitation variability in the YTR basin, and its potential impacts on water management and control of water disasters, is vital for the sustainable development of Tibet. Many studies have analyzed precipitation variability in the YTR basin by considering its linear trends [*Zhang et al*., 2003; *Xu et al*., 2006; *Lu et al*., 2008]. However, they did not evaluate the nonstationary and nonlinear variability of precipitation and did not clarify the spatial difference in precipitation variability either. More importantly, it is commonly known that hydroclimatic conditions in the YTR basin are mainly controlled by the Indian monsoon, and some studies also have suggested that different phases of the Indian monsoon may change the intensity of the South Asian High and the western North Pacific anticyclone in summer and hence variations of monsoon-induced rainfall over China [*Ding and Chan*, 2005], especially the YTR basin [*Yao et al*., 2013]. However, it remains unclear as to how precipitation variability in the YTR basin responds to the change in the Indian monsoon at different time scales. On the whole, present studies did not quantitatively investigate the relationship between the precipitation variability and the changing Indian monsoon, and the possible mechanisms which cause precipitation variability in the YTR basin were not clearly expounded.

The objective of this study therefore is to investigate the precipitation variability over the last four decades in the YTR basin, since this constitutes the first but important step for water resources management in the region and control of disasters due to mountain torrents. Specifically, three aspects of precipitation variability are pursued: (1) seasonal distribution of precipitation; (2) interannual variation of precipitation; and (3) spatiotemporal variation of precipitation extremes. Change in the intensity of the Indian monsoon during recent decades and its relationship with the nonstationary variability of precipitation are investigated.

2. Data and Methods

2.1. Study Area

The Yarlung Tsangpo River basin lies between 81°42′ ~ 96°54′E and 27°43′ ~ 31°12′N, with an area of 0.24 million km^2 (Figure 1). As the highest major river in the world, the Yarlung Tsangpo River originates from

the Angsi Glacier in western Tibet, flows through the South Tibet Valley, and then passes through the state of Arunachal Pradesh, India, with a length of approximate 2057 km. The basin is bounded by the Himalayas in the south and Kang Rinpoche and Nyenchen Tanglha mountains in the north. Along with the decrease in altitude, the surrounding vegetation in the basin changes from cold desert to arid steppe to deciduous scrub vegetation and ultimately changes to a conifer and rhododendron forest.

Climatic conditions in the basin vary with regions [*Li et al*., 2013]. Due to the influence of humid air current from the Indian Ocean, the south valleys of the river are warm and rainy with an average temperature of 8.6°C, and precipitation mainly occurs in the rainy season. The middle and lower reaches of the basin are covered with good soil and groves of well irrigated trees. It is home to 50% of the Tibet Autonomous Region's population (Shigatse, Lhasa, Lhoka, and Nyingchi Prefectures). Therefore, water resources in the river are important for the people of Tibet.

2.2. Data

Data on daily precipitation measured at eight weather stations were selected to analyze the precipitation variability in the YTR basin. The data were obtained from the China Meteorological Data Sharing Service System. The weather stations were selected by considering the length, consistency, and completeness of records. All the series have the same measurement years from 1973 to 2011, with no missing segments. There is no observation station in the upper reach of the river. Many stations are located around the basin (Shiquanhe, Burang, Gerze, etc.). However, the topographic, geographic, and hydroclimatic conditions have great differences in and around the YTR basin, so the precipitation measured at those stations around the basin cannot accurately reflect the precipitation conditions in the YTR basin, and these data cannot be used for our study. As a result, the precipitation variability in the middle and lower reaches of the river was analyzed using eight stations in the basin.

Data on the Indian summer monsoon (ISM) index were used to study the changes of the Indian monsoon. The data were obtained for measurement years from 1973 to 2011. The ISM typically lasts from June to September in a year, with large areas of the India Ocean region receiving more than 60% of their total annual precipitation during the period, and the largest precipitation values are observed during the heart of the monsoon season in July and August [*Wang and Fan*, 1999]. The intensity of ISM can be represented by the difference of the 850 hPa zonal winds between a southern region (40°E–80°E, 5 N–10 N) and a northern region (70°E–90°E, 20 N–30 N), called ISM index (ISMI) [*Wang et al*., 2001]. The definition reflects both the intensity of the tropical westerly monsoon and the lower tropospheric vorticity anomalies associated with the ISM trough. Changes in the ISM would influence the rainy season precipitation in the YTR basin [*Yao et al*., 2013], but their relationship has not been clearly understood.

2.3. Methods

Both the seasonal distribution and interannual nonstationary variability of precipitation in the YTR basin were analyzed, and their spatial differences were also considered. We employed the indices of concentration ratio (CR) and concentration period (CP) to investigate the seasonal distribution of monthly precipitation, applied the empirical mode decomposition (EMD) method to investigate the long-term nonstationarity of annual precipitation, and further used the detrended fluctuation analysis (DFA) method to investigate the scaling behavior of annual precipitation series in each station. Besides, daily precipitation with a magnitude of 25–50 mm/d (P25) and that bigger than 50 mm/d (P50), approximately reflecting storm rain and torrential rain, respectively, were analyzed to investigate the variation of precipitation extremes. Two indices, occurrence time and average magnitude, were used to describe the variation of precipitation extremes. Each method is described in the following, and all analyses were conducted in MathWorks MATLAB R2010a.

2.3.1. Computation of CR and CP

For computation of CR and CP it is assumed that monthly precipitation is a vectorial quantity with both magnitude and direction. One year is considered as a cycle of 360°, and the *i*th month corresponds to $\theta_i = 360°/12 \times i = 30° \times i$, with $i = 1, 2, \ldots, 12$. The resulting vector of monthly precipitation is expressed as

$$\mathrm{CR} = \sqrt{{R_x}^2 + {R_y}^2}/P_0;\ \ \mathrm{CP} = \arctan\left(R_x/R_y\right) \tag{1}$$

$$R_x = \sum_{i=1}^{12} P_i \times \sin(\theta_i);\ \ R_y = \sum_{i=1}^{12} P_i \times \cos(\theta_i), \tag{2}$$

where P_i is the precipitation in the ith month, and P_0 is the annual precipitation. With the value ranging between 0 and 1, a bigger CR value reflects a more concentrated degree of monthly precipitation in a year and vice versa. A CP value reflects the month in which monthly precipitation of a year mainly occurs.

2.3.2. EMD Method

The EMD method decomposes a series into a set of components called intrinsic mode functions (IMFs), being the basis for representing the series [*Huang et al*., 1998; *Kim and Oh*, 2008]. As the basis is adaptive, it usually offers a physically meaningful representation of the underlying process [*Kim and Oh*, 2009]. Therefore, EMD is ideally suitable for analyzing data from nonstationary to nonlinear processes [*Huang and Wu*, 2006]. EMD is implemented through an adaptively sifting process that uses only local extrema of a series. A series decomposed by EMD can be expressed as

$$x(t) = \sum_{i=1}^{N} C_i + R_N, \tag{3}$$

where N is the number of IMFs separated from series $x(t)$, C_i is the ith IMF, and R_N is the residual, which has the lowest frequency and generally corresponds to the series' trend. More mathematical details of EMD can be found in [*Huang and Wu*, 2006]. *Wu and Huang* [2004] established a method to evaluate the statistical significance of useful information contents for IMFs from any noisy data, and it was used here to evaluate the statistical significance of series' periodicities and trend.

2.3.3. DFA Method

The DFA method can explore the long-range correlations of a series [*Bashan et al*., 2008]. For a series with length L and the given scale s, it is first divided into segments of equal length s. In each segment of length s, a least squares line is fitted to the data, representing the trend in that segment. The y coordinate of the straight line segment is denoted by $x_s(k)$. The integrated time series $x(k)$ is detrended by subtracting the local trend $x_s(k)$ in each segment. The root-mean-square fluctuation of the integrated and detrended series is calculated by

$$F(s) = \sqrt{\frac{1}{L}\sum_{k=1}^{L}\left[x(k) - x_s(k)\right]^2}. \tag{4}$$

The computation is repeated over all time scales to characterize the relationship between $F(s)$ and scale s. A linear relationship on a log-log plot indicates the presence of power law (fractal) scaling, and the fluctuations can be characterized by a scaling exponent σ and the slope of the line relating log $F(s)$ to log s, which indicates the scaling behavior of precipitation process of concern in this study. Theoretically, an exponent σ of 0.5 would correspond to uncorrelated white noise, and an exponent σ being smaller (bigger) than 0.5 would correspond to anticorrelated (correlated) series. When considering the statistical significance at 95% confidence level [*Weron*, 2002], the precipitation series analyzed with the exponent σ of 0.46–0.53 is an uncorrelated white noise, and the precipitation series analyzed with the exponent σ of 0–0.46 (0.53–1) is an anticorrelated (correlated) series.

3. Results and Discussion

3.1. Seasonal Distribution of Precipitation

Seasonal distributions of precipitation at all eight weather stations were analyzed. Monthly precipitation, with a CR value range of 0.18–0.92 (Figure 2a), mainly occurred from May to September (Figure 2b). However, the seasonal distribution of precipitation exhibited remarkable differences over space. Considering the locations of eight weather stations, the YTR basin can be roughly divided into three regions following the CR results, called the west YTR (Gyangtse, Dangxung, Tsetang, Shigatse, and Lhasa stations), middle YTR (Nyingchi and Lhari stations), and east YTR (Bomi station), with the mean CR values of 0.8, 0.6, and 0.4, respectively. Correspondingly, the mean CP values in the three regions are the mid-June, early June, and May. Generally, the May to September period was determined as the rainy season in the YTR basin. The ratio between rainy season and annual precipitation in each year was computed (Figure 2c), which also shows the differences among the three regions. The rainy season precipitation in the west and middle regions accounts for more than 90% and 80% of annual precipitation, respectively, while the rainy season precipitation only accounts for 55% of annual precipitation in the east region.

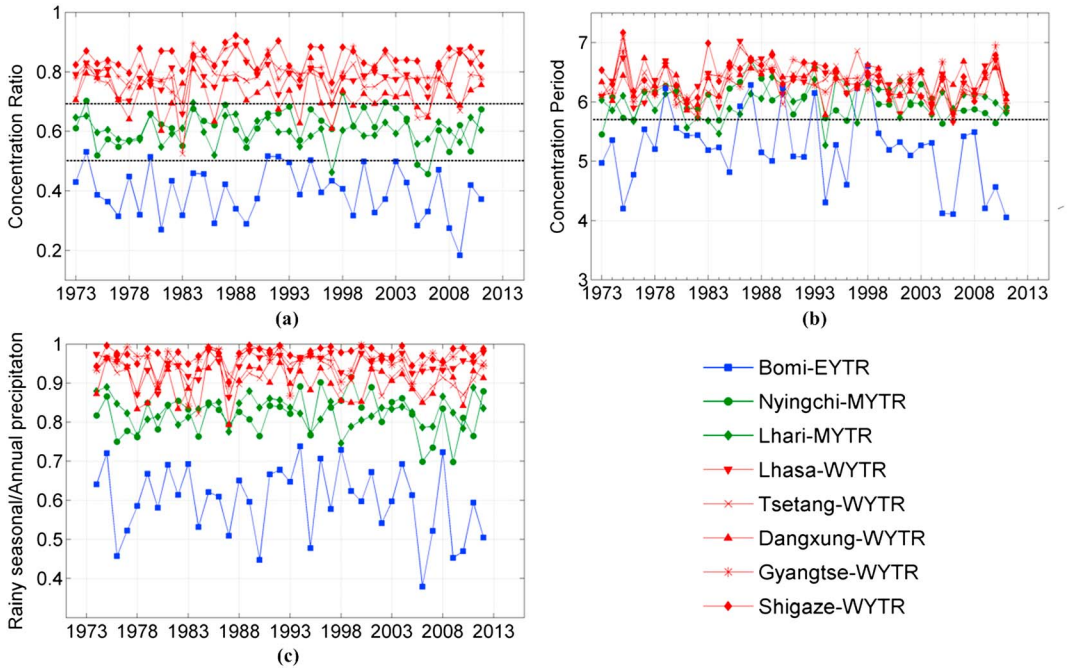

Figure 2. Results of the (a) concentration ratio (CR) and (b) concentration period (CP) of monthly precipitation, and the ratio between (c) rainy season precipitation to annual precipitation at the eight weather stations in the east (EYTR), middle (MYTR), and west (WYTR) Yarlung Tsangpo River (YTR) basin.

The monthly mean precipitation during the recent 39 years was analyzed. As shown in Figure 3, the seasonal distributions of precipitation in the three regions are notably different. The rainy season in the west region mainly concentrated on two months (July and August) and precipitation in the middle region mainly confined in 4 months (from June to September). In the east region, however, the seasonal timing of precipitation mainly occurred in 8 months (March to October). Results clearly reveal the spatial difference in the seasonal distribution of monthly precipitation in the basin. From downstream to upstream, the rainy season is delayed and becomes shorter, and the ratio of rainy season precipitation to annual precipitation increases, but the absolute magnitudes of rainy season precipitation and annual precipitation decrease.

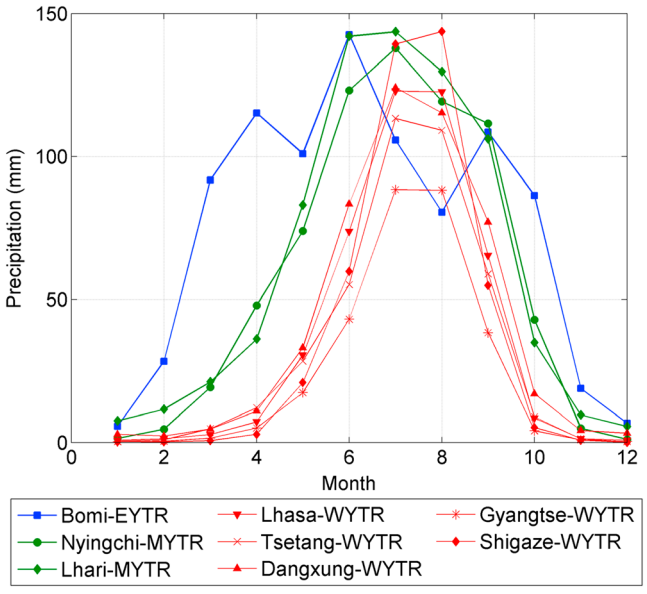

Figure 3. Average monthly precipitation processes in the east (EYTR), middle (MYTR), and west (WYTR) Yarlung Tsangpo River (YTR) basin.

3.2. Interannual Variation of Precipitation

Interannual variations of precipitation series were analyzed to investigate the nonstationary characteristics of precipitation. Figure 4a depicts the EMD-based decadal variability of annual precipitation, which shows similarity in the three regions. In the east region, the annual precipitation fluctuated and increased from 1973 to 1997 and decreased afterward. In the middle and west regions, the annual precipitation decreased during 1973–1983 and fluctuated during 1984–1997, during which precipitation on the whole showed an upward trend. After 1998, the annual precipitation manifested a decreasing trend in the

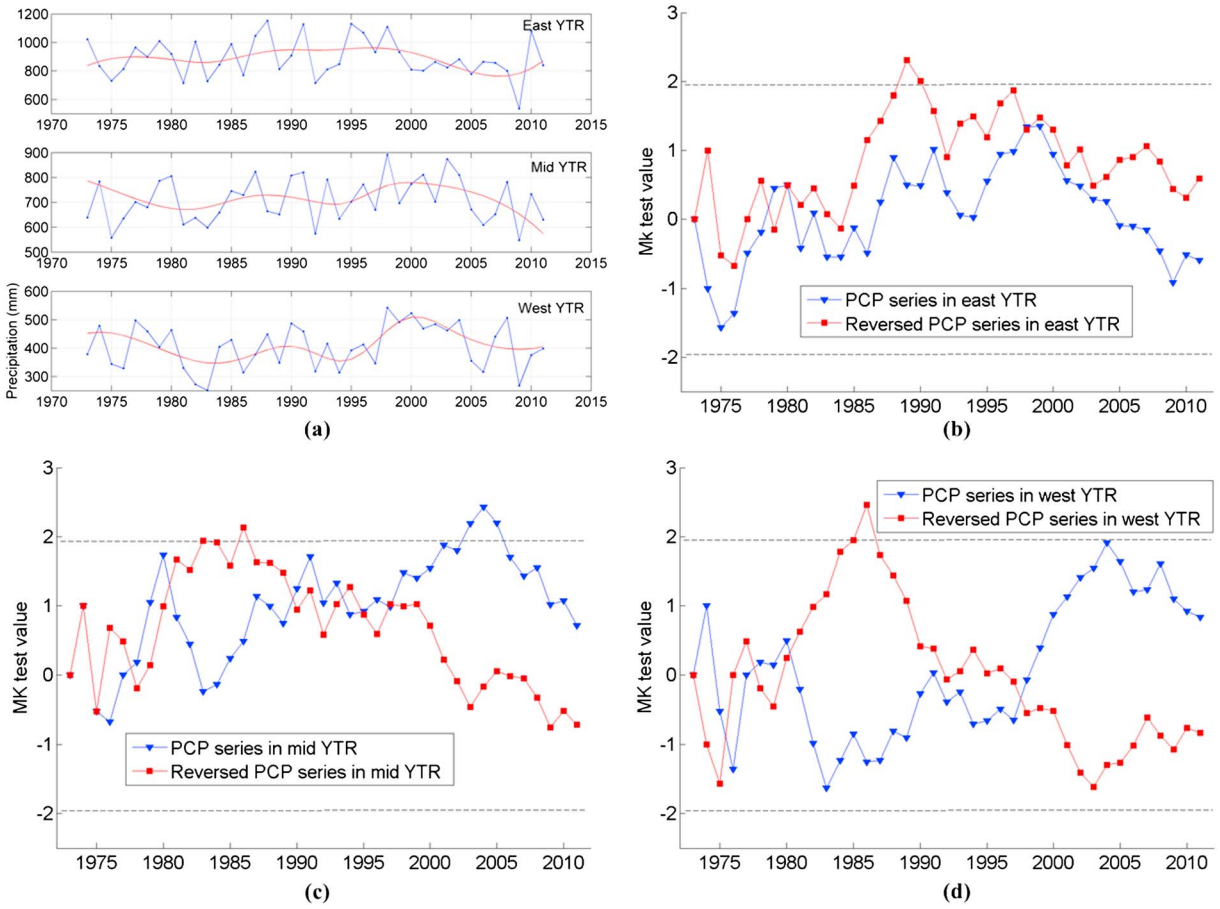

Figure 4. (a) The empirical mode decomposition (EMD) based nonlinear trends of annual precipitation and (b-d) the turning years of annual precipitation (PCP) identified by the Mann-Kendal (MK) test in the Yarlung Tsangpo River (YTR) basin.

middle and west regions. Additionally, results of the Mann-Kendal (MK) test identify the turning year of around 1980 and 1998 (Figures 4b–4d). Considering that the period 1973–1980 is too short to get reliable results, here we mainly consider the turning year of 1998, when three annual precipitation series have the biggest magnitudes in the whole period. As a result, the annual precipitation showed a downward trend after 1998 throughout the basin. Results in Figure 2c indicate that the ratio of rainy season precipitation to annual precipitation also decreased after 1998. Therefore, it is concluded here that the decrease of annual precipitation in the basin is mainly attributed to the decrease of rainy season precipitation. Besides, recent studies suggested that runoff process in the YTR basin is mainly controlled by the precipitation process, and the runoff process exhibited a downward trend since the late 1990s [*Liu et al.*, 2007; *Yang et al.*, 2014]. It indicates here that the precipitation decrease, especially the decrease in rainy season precipitation, causes a streamflow decrease in the Yarlung Tsangpo River after 1998.

The scaling behaviors of the precipitation series measured at eight stations were analyzed by the DFA method. The values of the scaling exponent σ of the eight series are similar (Figure 5). The precipitation series measured at the Lhari station owns the smallest scaling exponent value of 0.111, while the counterpart at the Gyangtse station has the biggest scaling exponent value of 0.222. Because all the scaling exponents are far smaller than 0.46, the precipitation processes in the YTR basin perform obvious long-memory characteristics but show anticorrelations at 95% confidence level. Besides, all the eight precipitation series have similar scaling behaviors, so it is thought that the middle and lower reaches of the YTR basin are controlled by the same climatic condition.

3.3. Spatiotemporal Variation of Precipitation Extremes

Spatiotemporal variations of the P25 and P50 precipitation extremes were analyzed to provide a potential guide for the control of disasters due to mountain torrents in the basin and Tibet. The P50 precipitation

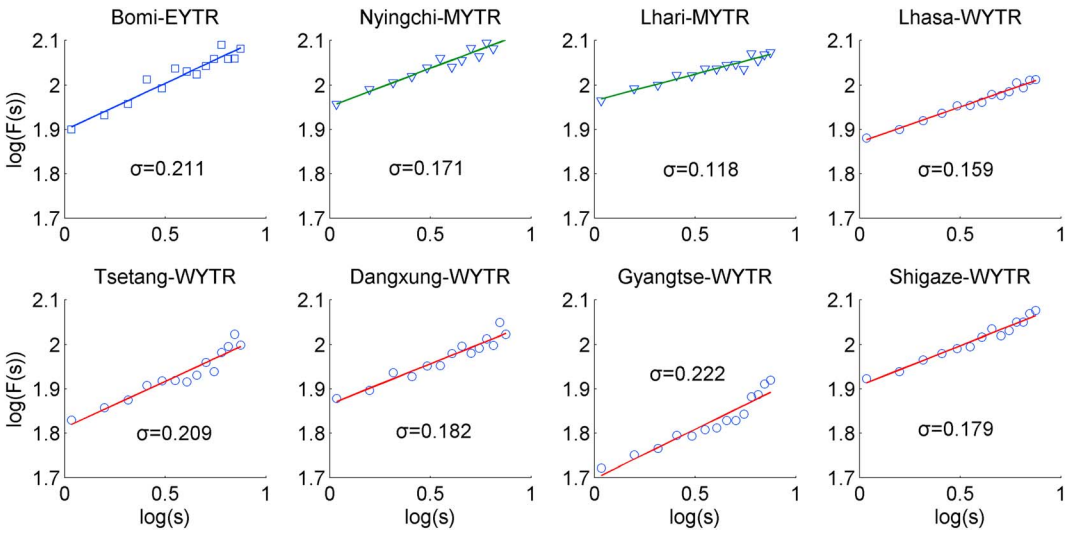

Figure 5. Results of scaling exponent of annual precipitation series at the eight weather stations in east (EYTR), middle (MYTR), and west (WYTR) Yarlung Tsangpo River (YTR) basin. The results are gotten by the detrended fluctuation analysis (DFA) method.

extremes just occurred 6 times at the Bomi station, with an average magnitude of 66.9 mm/d, and occurred only once at the Dangxung station, with a magnitude of 50.4 mm/d. Two stations are both located in the lower YTR basin. The P50 precipitation extremes did not occur at the other six stations. Due to the limited occurrence times of the P50 extremes, a trend could not be accurately estimated. Here the P25 precipitation extremes were of main concern.

The occurrence times and average magnitudes of the P25 extremes are also different in the three regions (Table 1). For the whole period, the P25 precipitation extremes occurred much more times at the Bomi station (i.e., east region) than at other stations (middle and east regions). From downstream to upstream, the occurrence times of P25 precipitation extremes reduced, except for the Shigatse station where more than 1.5 times the P25 precipitation extreme occurred per year. However, the average magnitudes of the P25 precipitation were similar at all eight stations, with the value ranging from 28.98 to 32.52 mm/d, and the average value of 30.77 mm/d. The *t* test results indicate that both the occurrence times and average magnitudes of the P25 precipitation extremes do not change between the two periods 1973–1997 and 1998–2011, except that the occurrence times of the P25 extremes significantly decrease at the Nyingchi station.

In order to further investigate the variability of the P25 precipitation extremes, the time series describing its occurrence times and average magnitudes were analyzed by the MK test to identify trends. Results in Table 2 indicate that both the occurrence times and average magnitude of the P25 extremes show downward trends

Table 1. Occurrence Times and Average Magnitudes of the P25 Precipitation Extremes During 1973–2011 in the Yarlung Tsangpo River Basin[a]

	Occurrence times (times per year)			Average magnitude (mm)		
Station	1973–1997	1998–2011	*t* test	1973–1997	1998–2011	*t* test
Bomi	4.41	2.92	–	32.52	31.51	–
Nyingchi	2.74	1.25	+	29.58	30.39	–
Lhari	1.59	1.75	–	30.51	29.81	–
Lhasa	1.07	1.08	–	31.08	32.37	–
Dangxung	0.81	1.08	–	31.70	29.80	–
Tsetang	1.04	1.17	–	29.52	28.98	–
Gyangtse	0.52	0.67	–	30.84	29.27	–
Shigaze	1.93	1.5	–	30.92	29.84	–

[a]For the *t* test results, the "+" means the significant difference of the value between the 1973–1997 and 1998–2011, and the "–" means no significant difference of the value between the 1973–1997 and 1998–2011.

Table 2. Statistical Significance of the Trend of the P25 Precipitation Extremes During 1973–2011 in the Yarlung Tsangpo River Basin[a]

	1973–2011		1973–1997		1998–2011	
Station	Occurrence times (times per year)	Average magnitude (mm)	Occurrence times (times per year)	Average magnitude (mm)	Occurrence times (times per year)	Average magnitude (mm)
Bomi	−1.34	−0.64	0.61	−0.14	0.49	0.27
Nyingchi	**−3.86**	−0.16	−1.82	0.89	−1.48	0.16
Lhari	**−2.89**	−0.30	**−2.62**	−1.87	**−2.14**	0.71
Lhasa	−1.00	−0.71	−0.19	−0.51	−0.60	0.05
Dangxung	**−3.06**	−1.42	**−2.80**	**−2.01**	−1.04	−1.15
Tsetang	−1.88	−1.10	**−2.06**	−1.68	−1.81	−1.48
Gyangtse	**−3.57**	**−4.66**	**−3.83**	**−2.74**	**−2.46**	−1.81
Shigaze	**−2.07**	−1.25	−1.07	−1.35	**−2.03**	−0.38

[a]The bold numbers highlight those statistically significant trends at 95% significance level.

during 1973–2011. Particularly, the occurrence times of the P25 precipitation extremes at the Nyingchi, Lhari, Dangxung, Gyangtse, and Shigaze stations show obviously downward trends at 95% significance level, and the average magnitudes of the P25 precipitation extremes at the Gyangtse station show obviously a downward trend at 95% significance level. Moreover, the results during 1973–1997 and 1998–2011 also indicate downward trends of the occurrence times of the P25 precipitation extremes, except the Bomi station in 1998–2011, although the downward trends at some stations are insignificant. The average magnitudes of the P25 precipitation extremes show downward trends at seven stations, with the exception of the Nyingchi station during 1973–1997, and at four stations (Dangxung, Tsetang, Gyangtse, and Gyangtse stations) during 1998–2011. On the whole, because the middle and lower reaches of the YTR basin have been encountering less P25 precipitation extremes along with years, it is favorable for the control of disasters due to mountain torrents.

4. Potential Influence of Climate Change on Precipitation Variation

The annual water vapor fluxes at the 500 hPa and 850 hPa levels show that air currents in the study area come from the south and west, respectively (Figure S1), reflecting the combined effects of westerlies and Indian monsoon at the annual scale. Because the influence of the Indian monsoon mainly occurs in summer [*Wang et al*., 2001], during which time more than 60% of the annual precipitation occurs, the water vapor fluxes from June to August are mainly considered. The water vapor fluxes both at the 500 hPa and 850 hPa levels in Figure 6 clearly display that the ISM brings significant amounts of warm and wet air currents from the Indian Ocean and comes to southeast Tibet and the YTR basin through the Bay of Bengal, so the climatic conditions and precipitation process in summer in the YTR basin are mainly controlled by the ISM. Presently, there have been limited studies about the quantitative relationship between the ISM and the precipitation variability in the basin. Our results show the differences in seasonal distribution and interannual nonstationary variation of precipitation in the three regions of the YTR basin, and the CR and CP values in these regions also vary over space. Here we attempt to explain the nonstationary variability of precipitation in the basin according to the changes of the ISM.

We choose the 1978, 1980, and 1994 as three typically strong ISM years, with the ISMI values being bigger than 1.5, and choose the 1974, 1987, and 2009 as three typically weak ISM years, with the ISMI values being smaller than −1.2. The difference of the water vapor fluxes between the strong and weak ISM years shows the decrease in water vapor fluxes at the weak ISM years (Figures 6c and 6f). The magnitudes of precipitation in the east, middle, and west YTR basin are 891.3 mm, 672.9 mm, and 365.7 mm in strong ISM years, corresponding to 888.9 mm, 651.7 mm, and 329.9 mm in weak ISM years, and the decrease ratio is 0.26%, 3.15%, and 9.79%, respectively. It suggests that the magnitudes of precipitation become smaller in weak ISM years due to the decrease in water vapor fluxes, especially in the middle and west YTR basin. Moreover, it can be found that the effect of the ISM strengthens from downstream to upstream, causing more decrease in precipitation upstream compared with downstream in the weak ISM years, and further leading to different seasonal distributions of precipitation in the three regions: the concentration degree of precipitation increases, the ratio of rainy season precipitation to annual precipitation increases, and the onset time of rainy season is delayed and the rainy season becomes shorter upward to the upstream.

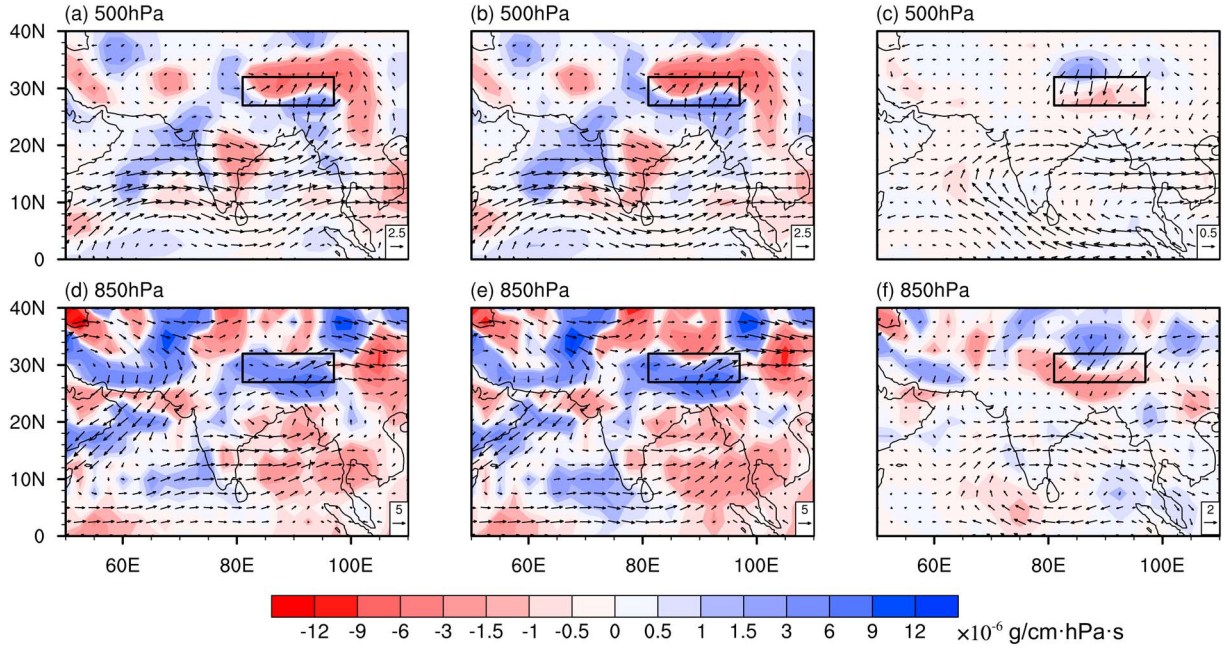

Figure 6. Water vapor fluxes in summer (June to August) composited from (a, d) three strong Indian summer monsoon (ISM) years: 1978, 1980, and 1994 and (b, e) three weak ISM years: 1974, 1987, and 2009 at the 500 hPa and 850 hPa levels. (c, f) The difference between the Figures 6b and 6e and 6a and 6d. The black box shows the region where the Yarlung Tsangpo River (YTR) basin is located in.

When considering the interannual variability of precipitation, periodicities of the ISMI series and summer precipitation are identified by spectral analysis. Results show the differences among the east, middle, and west YTR basin (Figure 7). The ISMI series exhibits 3–4, 7, and 11 year periodic variations. Correspondingly, all precipitation series in the east, middle, and west YTR basin show the 3–4 and 11 year periodic variations. The summer precipitation series in both the east and middle YTR basin show a 7 year periodic variation. However, the 7 year periodicity is not identified in the summer precipitation series in the west YTR basin. It can be due to the weak amplitude of the 7 year periodicity of ISMI, as the weakest one among the four periodicities, so the periodicity cannot affect the precipitation process in the west YTR basin, which is far from the Bay of Bengal. On the whole, from Figure 7 we can find that the interannual periodic variations of precipitation process in the YTR basin are basically controlled by the ISM.

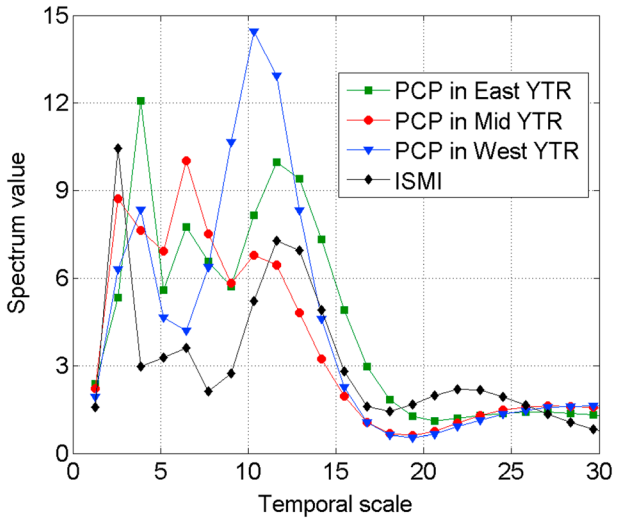

Figure 7. Spectra of the Indian summer monsoon index (ISMI) series and the summer precipitation (PCP) series during the period 1973–2011 in the Yarlung Tsangpo River (YTR) basin.

When considering the impact of climate change, recent studies have indicated the weakening Indian monsoon [*Wu*, 2005; *Thompson et al.*, 2006]. The weakening effects of the ISM can directly influence the precipitation variability in the YTR basin [*Naidu et al.*, 2009]. In order to confirm this observation of the weakening ISM and to investigate the relationship between the ISM and precipitation variability in the YTR basin, we used the EMD method to identify those useful information and describe the deterministic variability in the precipitation series and ISMI series (Figure 8). When considering 95% confidence level

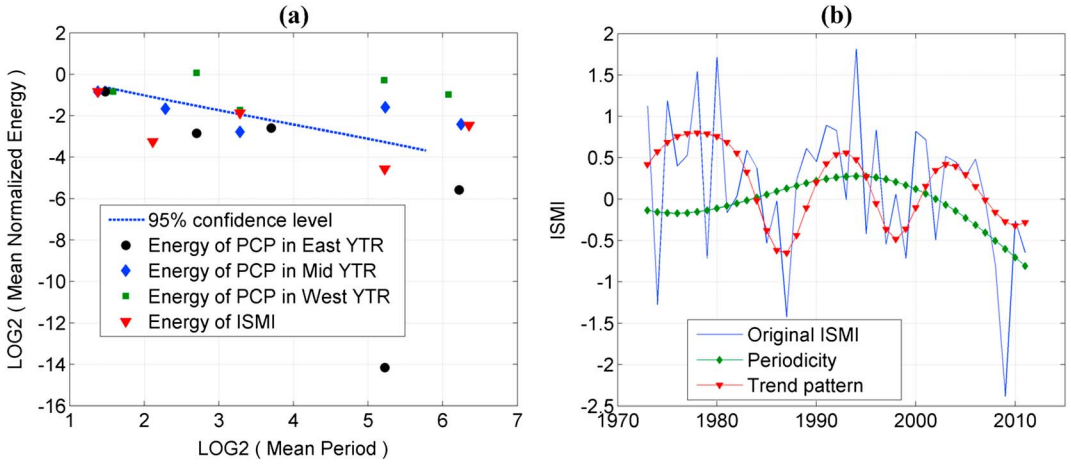

Figure 8. Significance test results of the Indian summer monsoon index (ISMI) series and the summer precipitation (PCP) series using the (a) EMD method and the periodicity and trend pattern identified in the (b) ISMI series.

(CL), all intrinsic mode functions (IFMs) of the precipitation series in the east YTR basin, with the energies being smaller than 95% CL, mainly show stochastic characteristics, and the decadal variability is not significant at 95% CL either. The fourth and fifth IMFs of the precipitation series in the middle YTR basin, with the energies being bigger than 95% CL, reflect the significantly decadal variability of the precipitation process, but the remaining IMFs mainly show stochastic characteristics. The fourth and fifth IMFs of the precipitation series in the west YTR basin, with the energies being bigger than 95% CL, reflect the significantly decadal variability of the precipitation process, and the second and third IMFs, with the energies being bigger than 95% CL, reflect the obviously periodic variability of the precipitation process, but the first IMF mainly shows stochastic characteristics. As for the ISMI series, its third and fifth IFMs reflect the periodic and trend pattern of the Indian summer monsoon, respectively, but other IMFs mainly show stochastic characteristics.

To quantify the relationship between the ISM and precipitation processes in the three regions of the YTR basin, we analyzed the partial correlations of the ISMI series and precipitation series in the whole period. The results gotten from original series, with the partial correlation coefficients of 0.18, −0.02, and −0.04 in the east, middle, and west YTR basin, are very small, and it can be due to the big influence of stochastic factors. We remove the stochastic components of each series and quantify the correlation of the ISMI and precipitation series again. They show significant correlations at 95% CL, with the partial correlation coefficients of 0.36, 0.56, and 0.81 in the east, middle, and west YTR basin. The relationship between the ISM and precipitation process becomes better from downstream to upstream, confirming again the strengthening effect of Indian monsoon upward to the upstream in the YTR basin.

Besides, from Figure 6 we know that if the Indian summer monsoon gets to be weakening, the ISMI value should decrease. Therefore, the ISMI and precipitation should have a positive relationship. Visually, the ISMI series has the biggest value at 1994 and then obviously decreases (Figure 8b), indicating the weakening effect of the ISM since the middle of 1990s. Following the trend pattern of the ISMI series (Figure 8b), here we roughly divide the ISMI series into two periods as those of precipitation. During the period 1973–1997, the ISMI series shows an upward trend, correspondingly, the precipitation series in the east and middle YTR show upward trends, with the increase rate of 2.8 mm/yr and 1.0 mm/yr, and the precipitation in the west YTR has no trend. The ISMI series indicates an obviously downward trend during the period 1998–2011. The precipitation in the east, middle, and west YTR basin also decreases during 1998–2011, with the decrease rate of −11.0 mm/yr, −13.0 mm/yr, and −11.0 mm/yr respectively. It is concluded here that precipitation decrease in the YTR basin is mainly caused by the weakening effect of the Indian summer monsoon during the recent two decades.

5. Conclusions

In the paper, the spatiotemporal variations of precipitation and precipitation extremes in the YTR basin are analyzed. The differences in precipitation over space are compared, and their relationships with the changing

Indian summer monsoon (ISM) are discussed. Results reflect that the seasonal distribution of precipitation varies spatially in the basin. From downstream to upstream, the rainy season is delayed and becomes shorter, and the ratio of rainy season precipitation to annual precipitation increases, but the absolute magnitudes of rainy season precipitation and annual precipitation decrease. It reflects the strengthening effect of the ISM upward to the upstream, based on which the basin can be roughly divided into east, middle, and west regions. Precipitation shows a downward trend after 1998. The decrease in annual precipitation is mainly caused by the decrease in the rainy season precipitation, which causes the river runoff to decrease in the basin. Both the occurrence times and average magnitudes of the P25 precipitation extremes exhibit downward trends, which is favorable for the control of disasters due to mountain torrents in the region.

Future changes in river streamflow and watershed hydrology caused by climate change are increasingly important for water resources management in Tibet [*Li et al*., 2014]. For the YTR basin, if the ISM keeps the presently weakening effect, water-related disasters in the region would more likely be reduced, but precipitation would keep a downward trend in the basin, the streamflow decrease in the river would continue, and potential water shortage situation in the region would become more severe. Therefore, proactive and effective adaptation strategies should be developed and implemented to cope with the unfavorable situation. In order to understand and evaluate the future precipitation variability in the YTR basin, more studies should focus on the mechanisms which cause the weakening Indian summer monsoon during recent decades; besides, the stochastic characteristics of the ISM and its potential influence on the precipitation variability in the YTR basin should also be further studied.

Acknowledgments

The authors gratefully acknowledged the valuable comments and suggestions given by the Editor, L. Ruby Leung, and the anonymous reviewers. The authors also thank Feifei Liu for her assistance in the preparation of the manuscript. The data were obtained from the China Meteorological Data Sharing Service System (http://cdc.cma.gov.cn/) and the website http://apdrc.soest.hawaii.edu/projects/monsoon/ismidx/ismidx-jja.txt. This project was financially supported by the Strategic Priority Research Program of the Chinese Academy of Sciences (XDB03030202), the National Natural Science Foundation of China (41330529 and 41201036), the Program for the "Bingwei" Excellent Talents from the Institute of Geographic Sciences and Natural Resources Research, Chinese Academy of Sciences, the Chinese Academy of Sciences Pioneer Hundred Talents Program, and the National Key Research and Development plan project (2016YFA0602402 and 2016YFC0401401).

References

An, Z., et al. (2012), Interplay between the Westerlies and Asian monsoon recorded in Lake Qinghai sediments since 32 ka, *Sci. Rep.*, *2*, 619, doi:10.1038/srep00619.

Bashan, A., R. Bartsch, J. W. Kantelhardt, and S. Havlin (2008), Comparison of detrending methods for fluctuation analysis, *Phys. A*, *387*, 5080–5090.

Bothe, O., K. Fraedrich, and X. H. Zhu (2011), Large-scale circulations and Tibetan Plateau summer drought and wetness in a high-resolution climate model, *Int. J. Climatol.*, *31*, 832–846.

Brunetti, M., M. Maugeri, F. Monti, and T. Nanni (2006), Temperature, precipitation variability in Italy in the last two centuries from homogenised instrumental time series, *Int. J. Climatol.*, *26*, 345–381.

Chandrasekar, V., R. Keranen, S. Lim, and D. Moisseev (2013), Recent advances in classification of observations from dual polarization weather radars, *Atmos. Res.*, *119*, 97–111.

Chen, M., D. Pollard, and E. J. Barron (2005), Hydrologic processes in China and their association with summer precipitation anomalies, *J. Hydrol.*, *301*, 14–28.

Ding, Y., and J. C. L. Chan (2005), The East Asian summer monsoon: An overview, *Moteorol. Atmos. Phys.*, *89*, 117–142.

Gao, J., V. Masson-Delmotte, T. Tao, C. Risi, and G. Hoffmann (2011), Precipitation water stable isotopes in the south Tibetan Plateau: Observations and modeling, *J. Clim.*, *24*, 3161–3178.

Huang, N. E., and Z. Wu (2006), A review on Hilbert-Huang transform: Method and its applications to geophysical studies, *Rev. Geophys.*, *46*, RG2006, doi:10.1029/2007RG000228.

Huang, N. E., Z. Shen, S. R. Long, M. L. C. Wu, H. H. Shih, Q. N. Zheng, N. C. Yen, C. C. Tung, and H. H. Liu (1998), The empirical mode decomposition method and the Hilbert spectrum for non-stationary time series analysis, *Proc. R. Soc. A-Math. Phys.*, *454A*, 903–995.

Kim, D., and H. S. Oh (2008), EMD: Empirical mode decomposition and Hilbert spectral analysis, URL http://cran.r-project.org/web/packages/EMD/index.html.

Kim, D., and H. S. Oh (2009), EMD: A package for empirical mode decomposition and Hilbert spectral analysis, *R. J.*, *1*, 40–46.

Klein, J. A., J. Harte, and X. Q. Zhao (2004), Experimental warming causes large and rapid species loss, dampened by simulated grazing, on the Tibetan Plateau, *Ecol. Lett.*, *7*, 1170–1179.

Li, C., and S. Kang (2006), Review of studies in climate change over the Tibetan Plateau, *Acta Meteorol. Sin.*, *61*, 327–335.

Li, F., Y. Zhang, and Z. Xu (2013), The impact of climate change on runoff in the southeastern Tibetau Plateau, *J. Hydrol.*, *505*, 188–201.

Li, F., Z. Xu, W. Liu, and Y. Zhang (2014), The impact of climate change on runoff in the Yarlung Tsangpo River basin in the Tibetan Plateau, *Stoch. Environ. Res. Risk Assess.*, *28*, 517–526.

Liu, J., Z. Yao, and C. Chen (2007), Evolution trend and causation analysis of the runoff evolution in the Yarlung Zangbo River basin [in Chinese with English Abstract], *J. Nat. Resour.*, *22*, 471–477.

Lu, H., Q. Shao, J. Liu, J. Wang, S. Chen, and Z. Chen (2008), Cluster analysis on summer precipitation field over Qinghai–Tibet Plateau from 1961 to 2004, *J. Geogr. Sci.*, *18*, 295–307.

Naidu, C. V., K. Durgalakshmi, K. Muni Krishna, S. Ramalingeswara Rao, G. C. Satyanarayana, P. Lakshminarayana, and L. Malleswara Rao (2009), Is summer monsoon rainfall decreasing over India in the global warming era? *J. Geophys. Res.*, *114*, D24108, doi:10.1029/2008JD011288.

Nie, N., W. C. Zhang, and C. Deng (2012), Spatial and temporal climate variations from 1978 to 2009 and their trend projection over the Yarlung Zangbo River basin, *J. Glaciol. Geocryol.*, *34*, 64–71.

Sang, Y. F., Z. Wang, Z. Li, C. Liu, and X. Liu (2012), Investigation into the daily precipitation variability in the Yangtze River Delta, China, *Hydrol. Process.*, *27*, 175–185.

Sang, Y. F., Z. Wang, C. Liu, and T. Gong (2013), Investigation into the climate variability in the headwater regions of the Yangtze River and Yellow River, China, *J. Clim.*, *26*(14), 5061–5071.

Shen, C. Y. (1986), *A Pandect of China Climate* [in Chinese], China Science Press, Beijing.

Thompson, L. G., E. Mosley-Thompson, H. Brecher, M. Davis, B. Leon, D. Les, P. N. Lin, T. Mashiotta, and K. Mountain (2006), Abrupt tropical climate change: Past and present, *Proc. Natl. Acad. Sci. U.S.A.*, *103*, 10,536–10,543.

Wang, B., and Z. Fan (1999), Choice of South Asian summer monsoon indices, *Bull. Am. Meteorol. Soc.*, *80*, 629–638.
Wang, B., R. Wu, and K. M. Lau (2001), Interannual variability of Asian summer monsoon: Contrast between the Indian and western North Pacific-East Asian monsoons, *J. Clim.*, *14*, 4073–4090.
Wang, C. (2013), Impact of anthropogenic absorbing aerosols on clouds and precipitation: A review of recent, *Atmos. Res.*, *122*, 237–249.
Wang, Y., E. Kromhout, C. Zhang, Y. Xu, W. Parker, T. Deng, and Z. Qiu (2008), Stable isotopic variations in modern herbivore tooth enamel, plants and water on the Tibetan Plateau: Implications for paleoclimate and paleoelevation reconstructions, *Palaeogeogr. Palaeocl.*, *260*, 359–374.
Wang, Z., Y. Ding, J. He, and J. Yu (2004), An updating analysis of the climate change in China in recent 50 years, *Acta Meteorol. Sin.*, *62*, 228–236.
Weron, R. (2002), Estimating long-range dependence: Finite sample properties and confidence intervals, *Phys. A*, *312*(1-2), 285–299.
Willems, P., K. Arnbjerg-Nielsen, J. Olsson, and V. T. V. Nguyen (2012), Climate change impact assessment on urban rainfall extremes and urban drainage: Methods and shortcomings, *Atmos. Res.*, *103*, 106–118.
Wu, B. (2005), Weakening of Indian summer monsoon in recent decades, *Adv. Atmos. Sci.*, *22*, 21–29.
Wu, Z., and N. E. Huang (2004), A study of the characteristics of white noise using the empirical mode decomposition method, *Proc. R. Soc. A-Math. Phys.*, *460*, 1597–1611.
Xu, B., et al. (2009), Black soot and the survival of Tibetan glaciers, *Proc. Natl. Acad. Sci. U.S.A.*, *106*, 114–122.
Xu, Z. X., T. L. Gong, and F. F. Zhao (2006), Analysis of climate change in Tibetan Plateau over the past 40 years, *J. Subtro. Resour. Environ.*, *1*, 24–32.
Xu, Z. X., T. L. Gong, and J. Y. Li (2008), Decadal trend of climate in the Tibetan Plateau-regional temperature and precipitation, *Hydrol. Process.*, *22*, 3056–3065.
Yang, Z., H. Zhuoma, C. Lu, P. M. Dava, and K. Zhou (2014), Characteristics of precipitation variation and its effects on runoff in the Yarlung Zangbo River basin during 1961–2010 [in Chinese with English abstract], *J. Glaciol. Geocryol.*, *36*, 166–172.
Yao, T. D., et al. (2012), Different glacier status with atmospheric circulation in Tibetan Plateau and surroundings, *Nat. Clim. Change*, *2*, 663–667.
Yao, T. D., et al. (2013), A review of climatic controls on $\delta^{18}O$ in precipitation over the Tibetan Plateau observations and simulations, *Rev. Geophys.*, *51*, 525–548, doi:10.1002/rog.20023.
Zhai, P. M., A. Sun, F. Ren, X. Liu, B. Gao, and Q. Zhang (1999), Changes of climate extremes in China, *Clim. Change*, *42*, 203–218.
Zhang, X., Y. Ren, Z. Y. Yin, Z. Lin, and D. Zheng (2009), Spatial and temporal variation patterns of reference evapotranspiration across the Qinghai-Tibetan Plateau during 1971–2004, *J. Geophys. Res.*, *114*, D15105, doi:10.1029/2009JD011753.
Zhang, Y. S., T. Ohata, and T. Kadota (2003), Land-surface hydrological processes in the permafrost region of the eastern Tibetan Plateau, *J. Hydrol.*, *283*, 41–56.